ADVANCED MATERIALS

www.advmat.de

Amorphizing of Cu Nanoparticles toward Highly Efficient and Robust Electrocatalyst for CO_2 Reduction to Liquid Fuels with High Faradaic Efficiencies

Yan-Xin Duan, Fan-Lu Meng, Kai-Hua Liu, Sha-Sha Yi, Si-Jia Li, Jun-Min Yan, and Qing Jiang*

Conversion of carbon dioxide (CO_2) into valuable chemicals, especially liquid fuels, through electrochemical reduction driven by sustainable energy sources, is a promising way to get rid of dependence on fossil fuels, wherein developing of highly efficient catalyst is still of paramount importance. In this study, as a proof-of-concept experiment, first a facile while very effective protocol is proposed to synthesize amorphous Cu NPs. Unexpectedly, superior electrochemical performances, including high catalytic activity and selectivity of CO_2 reduction to liquid fuels are achieved, that is, a total Faradaic efficiency of liquid fuels can sum up to the maximum value of 59% at −1.4 V, with formic acid (HCOOH) and ethanol (C_2H_6O) account for 37% and 22%, respectively, as well as a desirable long-term stability even up to 12 h. More importantly, this work opens a new avenue for improved electroreduction of CO_2 based on amorphous metal catalysts.

The continuously rising level of atmospheric carbon dioxide (CO_2), mainly caused by excessive emission from fossil fuel combustion and industrial production, has become one of the most severe worldwide problems.[1–3] In order to decrease the release of CO_2 and carry out carbon-neutral strategy, reducing CO_2 into fuels or high-value-added chemicals with the help of photocatalytic, chemical, and electroreductions is promising, which has attracted more and more research interests.[4–8] Compared with each other, electroreduction of CO_2 is highly competitive due to its controllability and the existing mature electrolytic technology and devices. Especially, when triggered by the electricity generated from renewable energy like wind and tide, a named "zero carbon cycle" can be reached.[9–11] Up to now, on the strength of various electrocatalysts and applied potentials, CO_2 can be converted to many kinds of products, including carbon monoxide (CO), methane (CH_4), ethylene (C_2H_4), formic acid (HCOOH), ethanol (C_2H_6O), etc.[12–18]

Y.-X. Duan, Dr. F.-L. Meng, K.-H. Liu, S.-S. Yi, S.-J. Li, Prof. J.-M. Yan, Prof. Q. Jiang
Key Laboratory of Automobile Materials
Ministry of Education
School of Materials Science and Engineering
Jilin University
Changchun 130022, China
E-mail: junminyan@jlu.edu.cn

The ORCID identification number(s) for the author(s) of this article can be found under https://doi.org/10.1002/adma.201706194.

DOI: 10.1002/adma.201706194

Among a series of reduction products, liquid products are highly desirable owing to their high energy density and easy transportation.[2,19,20] In which, HCOOH and C_2H_6O may be the most special ones in the reason of their enormous potential in electrochemical energy storage and conversion areas. For instance, HCOOH has attracted considerable interest in applications of fuel cell and hydrogen (H_2) storage for its high free energy of combustion (−233 kJ mol^{-1}) and theoretical H_2 gravimetric capacity (4.4 wt%; 53.4 g L^{-1}).[21–23] C_2H_6O is also being developed as a potential source for direct fuel cell, which is a promising alternative for conventional batteries.[24,25] Besides, both of them can be directly used in current infrastructures, therefore, synthesis of HCOOH and C_2H_6O through CO_2 electroreduction is of great interesting.

Cu-based materials are regarded as the unique one that can directly produce hydrocarbons and alcohols through CO_2 electroreduction, which have attracted much attention since early 1980s.[7,19,26,27] However, over most of these Cu-based catalysts for the generation of HCOOH and/or C_2H_6O, the selectivity (many gas products, such as CO, CH_4, and C_2H_4, are always generated together) and Faradaic efficiencies (FEs) (0–34%) (the heavy H_2 evolution competitive reaction) in aqueous media are still very ungratified (Table S1, Supporting Information). Despite unsatisfactory, in the development of improving selectivity and FEs of Cu-based catalysts, by adjusting the chemical states, surface modifications, and morphologies, different strategies have been adopted.[28–33] It should be noted that, all the attentions and factors have been focused on the crystalline Cu-based catalysts. Compared to crystalline materials, the amorphous ones generally have a large of low-coordinated atoms and hence abundant defects, thus, more catalytic centers are expected to be created for enhanced electrochemical performance.[34–37] In addition to that, amorphizing of the materials will cause the formation of "dangling bonds" that may provide more reactive sites, and as a result, improving the activity even selectivity for CO_2 reduction.[14,38,39] Therefore, it will be full of potentiality to prepare amorphous Cu catalyst to increase the catalytic selectivity and activity for CO_2 electroreduction toward liquid fuels of HCOOH and C_2H_6O.

Conventionally, the synthesis of amorphous Cu-based materials still heavily rely on techniques such as jet molding, composite explosive welding and mechanical alloying, laser electrodeposition, arc-melting pure metals under argon atmosphere, etc., which may have more or less shortcomings such as laborious and time-consuming process, requirement of special and expensive instrument. Even though, the obtained materials are typically in bulk structures, leading to large particle size, small specific surface area, and thus insufficient active sites as well as limited diffusion of substrate, which is intrinsically incapable for CO_2 electroreduction.[40,41] Up to now, there is no report on synthesis of amorphous and highly dispersed clean Cu nanoparticles (NPs), to say nothing of application as novel electrocatalyst with good conductivity and sufficient reactive sites for CO_2 electroreduction, moreover the amorphous Cu is in a metastable state with compared to its crystalline one, so the preparation of it remains face with serious challenge.[38,42] Therefore, developing a facile approach to synthesize amorphous Cu NPs and then explore their catalytic activity is highly desirable while still very challenging.

Herein, as a proof of concept, we first propose and demonstrate a facile while very effective protocol to synthesize amorphous Cu (a-Cu) NPs using a very weak reducing environment at room temperature. Unexpectedly, when employed for CO_2 electroreduction in aqueous $KHCO_3$ solution, the a-Cu exhibits much well activity and selectivity for liquid fuels at −1.4 V versus Ag/AgCl (all further potentials discussed in the following are vs Ag/AgCl), and the FE for liquid products of HCOOH and C_2H_6O could rise up to 37% and 22%, respectively, with the formation of small amount of CO (5.8%), the total FE of CO_2 electroreduction achieves to 65% compared to the opposite crystallographic one. Such enhanced catalytic features on a-Cu are ascribed to the enhanced CO_2 adsorption ability, large active surface, and high mass transfer coefficient, which should be attributed to the abundant defect sites arising from intrinsic irregular atom structures of amorphous materials.

As illustrated in **Figure 1**a, the catalysts of a-Cu and c-Cu can be synthesized by direct reduction methods using different reducing agents at room temperature. Briefly, with the assistance of a tender reducing agent of tannic acid (TA), $CuCl_2$ could be reduced to a-Cu, when replaced with a strong reducing agent of sodium borohydride ($NaBH_4$), the reduced product is its opposite crystallographic one (c-Cu). The X-ray diffraction (XRD) patterns of the as-synthesized specimens of a-Cu and c-Cu presented in Figure 1b provide the evidences. Wherein, a-Cu shows the typical amorphous state with no diffraction peak, while c-Cu exhibits good crystallinity with obvious crystalline peaks at 43.4°, 50.5°, and 74.2°, which can be assigned to the (111), (200), and (220) planes of metallic Cu (JCPDS: 85-1326), respectively. In order to further identify a-Cu as metal copper, the X-ray photoelectron spectroscopy (XPS) analysis is then performed. The high-resolution Cu 2p XPS spectra (Figure 1c) indicate that the chemical state of Cu in a-Cu is metallic Cu^0 as well as c-Cu (Cu $2p_{3/2}$ and Cu $2p_{1/2}$ are located at 932.5 and 952.3 eV, respectively).[28,43,44] In addition, transmission electron microscopy (TEM) images of a-Cu (**Figure 2**a) and c-Cu (Figure 2b) show that these two specimens have similar particle sizes (the average sizes for a-Cu and c-Cu are 3.33 and 3.40 nm, respectively). The high-resolution TEM (HRTEM) image (inset

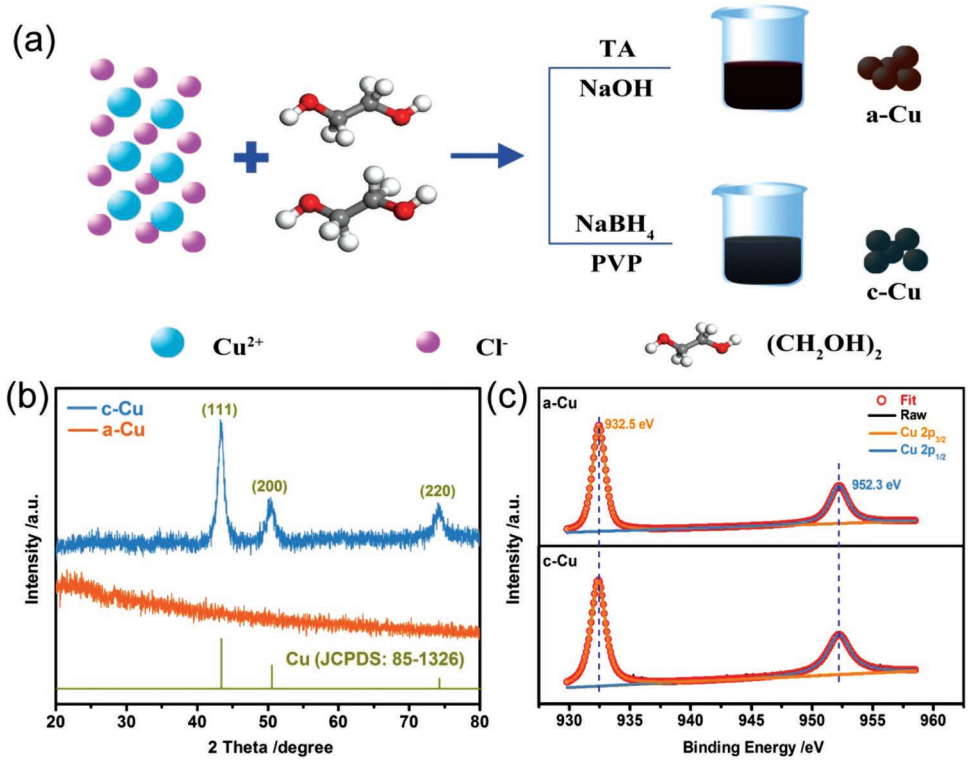

Figure 1. a) Schematic illustration for the formation process of a-Cu and c-Cu. b) XRD patterns and c) Cu 2p XPS spectra of a-Cu and c-Cu.

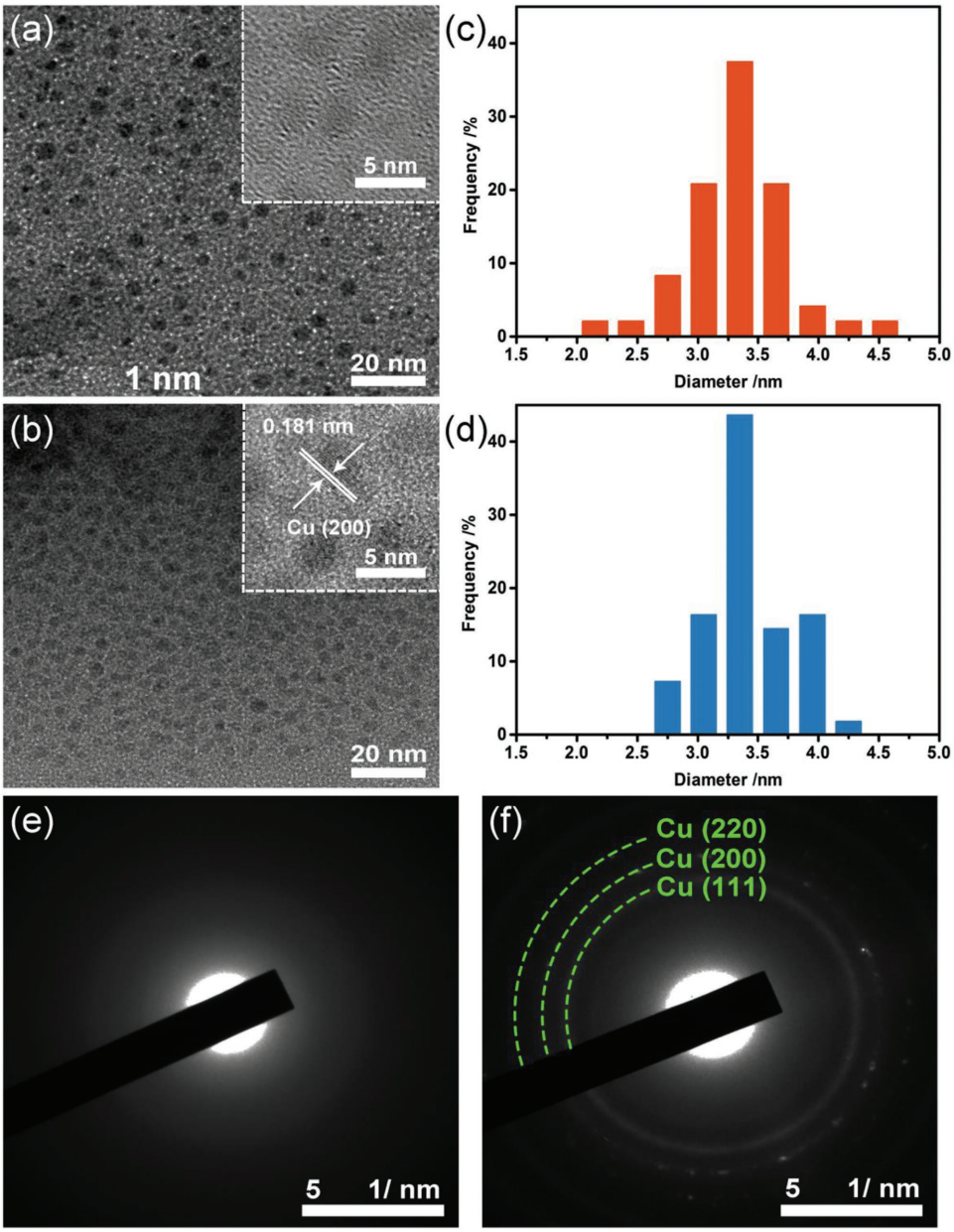

Figure 2. a,b) TEM image, c,d) size distribution, and d,e) SAED patterns of a-Cu and c-Cu, the insets in panels (a) and (b) are the HRTEM images of a-Cu and c-Cu, respectively.

of Figure 2a) of a-Cu exhibits the amorphous nature, while the image of c-Cu (inset of Figure 2b) reveals a lattice spacing of about 0.181 nm for c-Cu, corresponding to (200) plane of Cu, which are well consistent with the XRD results. Moreover, the corresponding selected area electron diffraction (SAED) patterns prove the amorphous feature of a-Cu with very ambiguous diffuse halo ring (Figure 2e), and the crystalline c-Cu with very distinct rings (Figure 2f),[45–47] agrees very well with their XRD results (Figure 1b).

To evaluate the performance of a-Cu and c-Cu as CO_2 reduction catalysts, both of them are loaded onto carbon cloth to serve as working electrodes. The single reductive linear sweep voltammetry (LSV) is first measured in Ar- and CO_2-saturated 0.1 M $KHCO_3$ aqueous solution using a three-electrode setup, which consists of cathodic and anodic compartments, separated by a Nafion 117 proton exchange membrane. As shown in **Figure 3**a, a quite difference happens to the LSV curves of a-Cu between the Ar- and CO_2-saturated electrolytes, the greatly improved current density in the presence of CO_2 compared to Ar should be attributed to the occurrence of the CO_2 electroreduction besides H_2 evolution reaction, which provides a direct evidence for the reduction of CO_2.[48,49] The c-Cu presents a similar situation. However, while fairly comparable in size and form, compared to the crystallized c-Cu, the amorphous a-Cu not only has much higher cathodic current density at potentials more negative than –0.8 V after the electrolyte is saturated

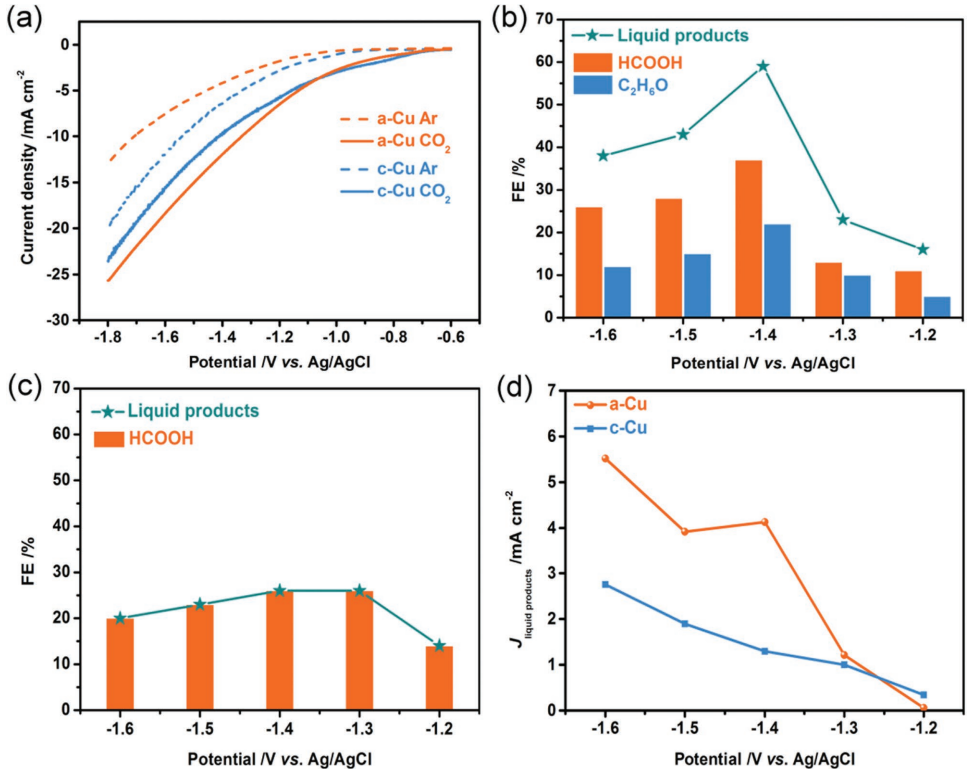

Figure 3. Catalytic performance of a-Cu and c-Cu. a) Single reductive LSV results in Ar-saturated (dashed line) and CO_2-saturated (solid line) 0.1 M $KHCO_3$ solution with a 50 mV s^{-1} scan rate. b,c) FE of liquid products at each given potential for 2 h. d) Partial current densities for the production of liquid products.

with CO_2 but also exhibits lower cathodic current density in the Ar condition, meaning great better catalytic activity toward CO_2 reduction of a-Cu. Such a sharp different increase degree between a-Cu and c-Cu implies that, the amorphization may be an efficient method for a much higher activity of electroreduction of CO_2.

To further get the product distribution of CO_2 reduction and analyze the selectivity of both a-Cu and c-Cu, the electrolysis is conducted at a variety of constant potentials from −1.0 to −1.6 V for 2 h in CO_2-saturated aqueous 0.1 M $KHCO_3$ solution at the ambient temperature and pressure on both two electrodes, subsequently (Figure S1, Supporting Information). Liquid products are quantified by nuclear magnetic resonance analysis after the electrolysis is finished. The cathodic compartment is purged with CO_2 constantly and vented directly into the gas-sampling loop of a gas chromatograph to examine the amount of gaseous products. The results shown in Figure 3b reveal that, a-Cu shows excellent selectivity for liquid products including HCOOH and C_2H_6O, which can reach the maximum FE of 37% and 22% at −1.4 V, respectively, very competitive compared with that of all the Cu-based catalysts listed in Table S1 (Supporting Information) (the highest FE for the liquid products). In addition, the carbon balance, determined by summing all of the carbon distributed in the products and dividing by initial carbon content introduced from the reactants, is calculated to be over 99.8%. The 0.2% difference might be attributed to the undetectable minor-products. In contrast, the highest FE of HCOOH over c-Cu is 26% at −1.4 V (Figure 3c), and C_2H_6O can only be detected at potentials more negative than −1.6 V, with the FE of just 6% at −1.7 V (Figure S2, Supporting Information). Apart from the competitive production of H_2, only small amount of gas product is detected from CO_2 reduction on a-Cu, including CO (5.8%) at −1.4 V, CH_4 (1%) and even C_2H_2 (5%) at −1.6 V (Figures S3 and S4, Supporting Information). The difference in selectivity for liquid products could be better visualized by plotting the partial current densities (Figure 3d). In addition, the electrolysis over a-Cu at −1.4 V in Ar-saturated 0.1 M $KHCO_3$ solution is conducted as well (Figure S5, Supporting Information), no production of liquid fuels is detected, further proving the reduction of CO_2.

The remarkably enhanced activity of a-Cu is partly ascribed to the high electrochemical active area (ECSA), which represents the amount of active sites to a certain degree, normally, the ECSA could be approximated to the electrochemical double layer capacitance (EDLC).[14,50] Cyclic voltammetry measurements are then performed in Ar-saturated electrolyte to determine the EDLC (Figure S6, Supporting Information). Not surprisingly, a-Cu exhibits a higher EDLC than c-Cu, indicating larger ECSA (**Figure 4**a), followed by a great number of active sites on a-Cu, which is an important contributor to the enhanced activity. As another key contributor, the kinetic of charge transfer (efficient charge transfer at the catalysts/electrolyte interface can facilitate the catalytic process) is then evaluated by electrochemical impedance spectroscopy measurements. As shown in Figure S7 (Supporting Information), semicircles appear in the front part of curves, of which, the

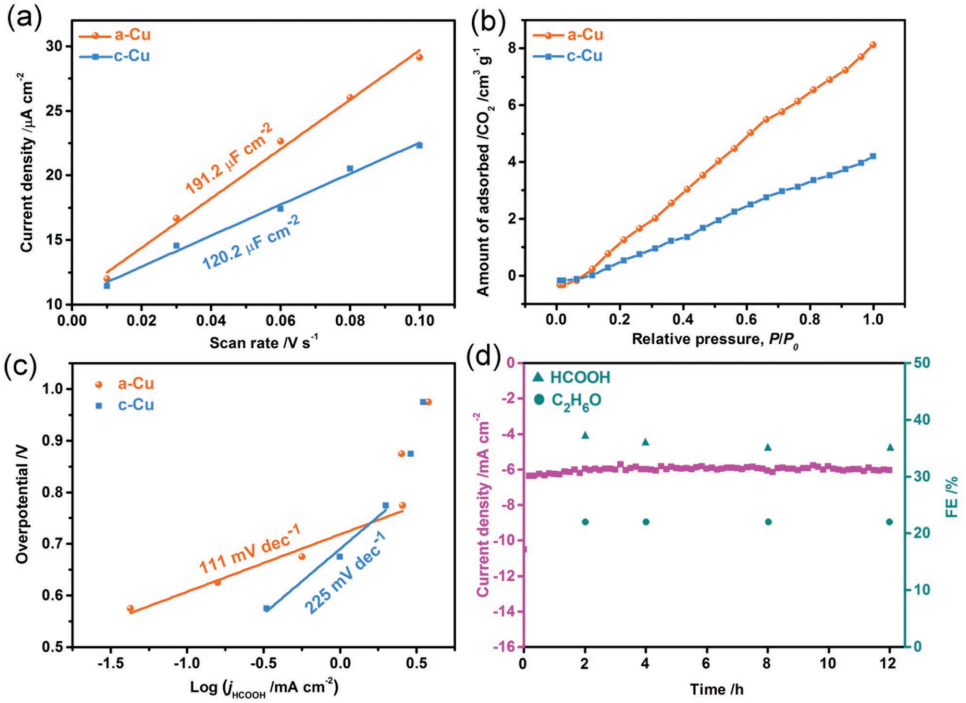

Figure 4. a) Current density plots at various scan rates of two electrodes, in which the figures illustrated are specific capacitance of a-Cu and c-Cu. b) CO_2 adsorption isotherms for two electrodes. c) Tafel plots for the HCOOH production on a-Cu and c-Cu, where j_{HCOOH} is the partial current density of HCOOH. d) Stability study of the a-Cu: at a constant potential of −1.4 V in a CO_2-saturated 0.1 M $KHCO_3$ solution. Current density (line) and FE (dots) of HCOOH and C_2H_6O during long-term operation (12 h) are illustrated, respectively.

semicircle radius of a-Cu is much smaller than that of c-Cu, which is related to faster charge transfer at the catalysts/electrolyte interface

$$CO_{2(g)} \rightarrow CO_2^* \quad (1)$$

$$CO_2^* + e^- \rightarrow CO_2^{*-} \quad (2)$$

$$CO_2^{*-} + H^+ + e^- \rightarrow HCOO^{*-} \quad (3)$$

$$HCOO^{*-} \rightarrow HCOO^-_{(aq)} \quad (4)$$

In general, an increased CO_2 adsorption could constantly provide raw materials (CO_2) for subsequent CO_2 reduction, which plays an important role in improving the catalytic ability of CO_2 reduction. The measurement of CO_2 adsorption amount is then carried out, Figure 4b reveals that a-Cu could adsorb fourfold amount of CO_2 than c-Cu. To further observe the insights into the mechanism pathway for electroreduction of CO_2 to HCOOH on the a-Cu, the Tafel slope for HCOOH production is measured (Figure 4c). The Tafel plots show a slope of 111 mV dec^{-1} for a-Cu. It is commonly assumed that, the production scheme of HCOOH (or formate) is illustrated in Equations (1)–(4).[14,51,52] After CO_2 is dissolved into the electrolyte and formed adsorbed CO_2 on the surface of the electrode (Equation (1)), the adsorbed CO_2 is initially reduced to the CO_2^{*-} by obtaining an electron (e^-) (Equation (2)), where the asterisk denotes an active site. Subsequently, the CO_2^{*-} intermediate is protonated by the proton transfer from HCO_3^- and the second e^- would be transferred from the electrode to form adsorbed $HCOO^{*-}$ (Equation (3)), resulting in the production of HCOOH (or formate) (Equation (4)). As for electroreduction of CO_2, the Tafel slope is a very valuable parameter to investigate the reduction reaction mechanism. It is generally believed that, there are two possible rate-determining steps (RDS) of CO_2 electroreduction favored by previous works.[14,52] A Tafel slope of 118 mV dec^{-1} supports that the one RDS for CO_2 electroreduction is the formation of CO_2^{*-} intermediate by the initial e^- transfer step (Equation (2)). In comparison, the slope of 59 mV dec^{-1} indicates that another RDS is the protonation of CO_2^{*-} (Equation (3)).[53,54] In our work, the obtained Tafel slope for HCOOH of 111 mV dec^{-1} implies the initial single e^- transfer step, which is illustrated by Equation (2), is the RDS of HCOOH for CO_2 reduction on a-Cu. In the case of C_2H_6O production over a-Cu, a slope of 216 mV dec^{-1} (Figure S8, Supporting Information) illustrates that, it shares the same RDS with HCOOH (Equation (2)).[47] The production steps of C_2H_6O share the same first two steps with HCOOH. After that, the adsorbed intermediates COOH* ($CO_2^{*-} + H^+ \rightarrow$COOH*) and CO* (COOH* + $H^+ + e^- \rightarrow$ CO* + H_2O) are produced by proton–electron transfer. Subsequently, CO* is further dimerized (2CO* + $H^+ + e^- \rightarrow C_2H_nO_2$*) or hydrogenated (CO* + $H^+ + e^- \rightarrow$ CHO*/COH*, 2CHO*/COH* + $H^+ + e^- \rightarrow C_2H_nO_2$*) to form $C_2H_nO_2$*, which could be ultimately reduced to C_2H_6O ($C_2H_nO_2$*+ $H^+ + e^- \rightarrow C_2H_6O$).[52,55] In addition, the Tafel slope for HCOOH on c-Cu is also measured (Figure 4d), and it shows the same RDS with that on a-Cu with a larger value of 225 mV dec^{-1}, furthermore, the smaller Tafel

slope implies better catalytic activity of a-Cu. The intermediates covered on the surface and mass transport are regarded as elements that could have a remarkable effect on Tafel slope. Moreover, at relatively negative potentials, mass transport of reactants and products between the electrode surface and electrolyte may have a negative effect on the measurement.[53,56]

The higher activity and superior performance of a-Cu are ascribed to the larger ECSA and enhanced CO_2 adsorption, which may originate from the abundance of self-optimized active sites generated from the intrinsic chemical heterogeneity and special electronic structure on the amorphous surface of a-Cu.[57] It is supposed that, the reactive sites during the regularly arranged atoms in short-range order are capable of binding and stabilizing the key CO* intermediates to some extent, which can facilitate the production of liquid fuels.[52]

In addition, the stability is a significant property in the practical applications of CO_2 reduction as well. In order to confine the stability of a-Cu, the electrolysis is conducted by a long-term operation at −1.4 V in aqueous 0.1 M $KHCO_3$ solution with the bubbled CO_2 (Figure S9, Supporting Information). During the beginning 4 h, the amount of HCOOH and C_2H_6O are detected once every 2 h. Next, the amount is detected every 4 h. And the $KHCO_3$ solution is continuously utilized for the whole 12 h without replacement. It is noteworthy in Figure 4d, the FE to HCOOH production shows a slight decrease after ≈4 h, which may be due to the higher coverage of the $HCOO^-$ on the surface of a-Cu, resulting from the growing concentrations of the products in the cathodic reactor. Nevertheless, the FE to HCOOH can maintain around 35% during the latter 8 h reduction reaction. In the previous work, the decay in FE of CO_2 reduction could be regained by replacing the electrolyte with a new one.[58] In general, the FE to HCOOH and C_2H_6O production remains about 35% and 22%, and the current density is still stable with no apparent decay over 12 h, indicating the good stability of a-Cu. The negligible change in XRD (Figure S10, Supporting Information) and TEM characterization (Figure S11, Supporting Information) during the constant-potential electrolysis indicates the favorable stability of a-Cu, which is further confirmed by the LSV results (Figure S12, Supporting Information). Thus, the a-Cu shows the potential to be a desirable catalyst for CO_2 electroreduction with high electrocatalyst activity and stability. In contrast, the characterized XRD (Figure S13, Supporting Information), TEM (Figure S14, Supporting Information), and LSV (Figure S15, Supporting Information) results of c-Cu after long-term operation change a lot, which undoubtedly illustrate the poor stability of c-Cu.

In summary, as a proof-of-concept experiment, we first propose and demonstrate a facile while effective strategy to significantly improve the catalytic activity and selectivity of electroreduction of CO_2 to liquid fuels, wherein amorphous Cu catalyst (a-Cu) with fine particle size, larger ECSA, enhanced CO_2 adsorption ability obtained at room temperature plays the crucial role. Importantly, selectivity for liquid fuels in aqueous 0.1 M $KHCO_3$ solution, with the peak FE to HCOOH and C_2H_6O are 37% and 22% at −1.4 V, and the total FE of CO_2 reduction could reach up to the maximum value of 65%. Furthermore, a-Cu exhibits a desirable stability over 12 h. Amorphizing of Cu catalyst is a promising way for electroreduction of CO_2 to other valuable liquid fuels, and amorphous catalysts could be easily extended to other scientifically and technologically important energy conversion/storage reactions such as O_2/N_2 electroreduction.

Supporting Information

Supporting Information is available from the Wiley Online Library or from the author.

Acknowledgements

Y.-X.D. and F.-L.M. contributed equally to this work. This work was financially supported in part by the National Natural Science Foundation of China (Grant Nos. 51522101, 51631004, and 51471075); Program for JLU Science and Technology Innovative Research Team (2017TD-09); and the Fundamental Research Funds for the Central Universities.

Conflict of Interest

The authors declare no conflict of interest.

Keywords

amorphous Cu, CO_2 electroreduction, liquid fuels, selectivity

Received: October 25, 2017
Revised: November 30, 2017
Published online: February 23, 2018

[1] F. Lei, W. Liu, Y. Sun, J. Xu, K. Liu, L. Liang, T. Yao, B. Pan, S. Wei, Y. Xie, *Nat. Commun.* **2016**, *7*, 12697.
[2] F. Li, L. Chen, M. Xue, T. Williams, Y. Zhang, D. R. MacFarlane, J. Zhang, *Nano Energy* **2017**, *31*, 270.
[3] A. Rabiee, D. Nematollahi, *Mater. Chem. Phys.* **2017**, *193*, 109.
[4] H. Takeda, K. Ohashi, A. Sekine, O. Ishitani, *J. Am. Chem. Soc.* **2016**, *138*, 4354.
[5] I. Omae, *Coordin. Chem. Rev.* **2012**, *256*, 1384.
[6] A. Eilert, F. Cavalca, F. S. Roberts, J. Osterwalder, C. Liu, M. Favaro, E. J. Crumlin, H. Ogasawara, D. Friebel, L. G. Pettersson, A. Nilsson, *J. Phys. Chem. Lett.* **2017**, *8*, 285.
[7] H. Mistry, A. S. Varela, C. S. Bonifacio, I. Zegkinoglou, I. Sinev, Y. W. Choi, K. Kisslinger, E. A. Stach, J. C. Yang, P. Strasser, B. R. Cuenya, *Nat. Commun.* **2016**, *7*, 12123.
[8] M. F. Baruch, J. E. Pander, J. L. White, A. B. Bocarsly, *ACS Catal.* **2015**, *5*, 3148.
[9] D. Bogdanov, C. Breyer, *Energy Convers. Manage.* **2016**, *112*, 176.
[10] M. Bhattacharya, S. R. Paramati, I. Ozturk, S. Bhattacharya, *Appl. Energy* **2016**, *162*, 733.
[11] S. Kumar, G. Pal, T. Shah, *J. Cleaner Prod.* **2017**, *145*, 180.
[12] Z. Weng, J. Jiang, Y. Wu, Z. Wu, X. Guo, K. L. Materna, W. Liu, V. S. Batista, G. W. Brudvig, H. Wang, *J. Am. Chem. Soc.* **2016**, *138*, 8076.
[13] F. Quan, D. Zhong, H. Song, F. Jia, L. Zhang, *J. Mater. Chem. A* **2015**, *3*, 16409.
[14] S. Gao, Y. Lin, X. Jiao, Y. Sun, Q. Luo, W. Zhang, D. Li, J. Yang, Y. Xie, *Nature* **2016**, *529*, 68.
[15] F. Li, S. F. Zhao, L. Chen, A. Khan, D. R. MacFarlane, J. Zhang, *Energy Environ. Sci.* **2016**, *9*, 216.
[16] Y. J. Zhang, A. A. Peterson, *Phys. Chem. Chem. Phys.* **2015**, *17*, 4505.

[17] W. Lv, J. Zhou, J. Bei, R. Zhang, L. Wang, Q. Xu, W. Wang, *Appl. Surf. Sci.* **2017**, *393*, 191.
[18] R. Hinogami, S. Yotsuhashi, M. Deguchi, Y. Zenitani, H. Hashiba, Y. Yamada, *ECS Electrochem. Lett.* **2012**, *1*, H17.
[19] T. Cheng, H. Xiao, W. A. Goddard, *J. Am. Chem. Soc.* **2016**, *138*, 13802.
[20] S. Zhang, P. Kang, T. J. Meyer, *J. Am. Chem. Soc.* **2014**, *136*, 1734.
[21] J. Wu, F. G. Risalvato, F. S. Ke, P. J. Pellechia, X. D. Zhou, *J. Electrochem. Soc.* **2011**, *159*, 353.
[22] D. Mellmann, P. Sponholz, H. Junge, M. Beller, *Chem. Soc. Rev.* **2016**, *45*, 3954.
[23] K. Mori, S. Masuda, H. Tanaka, K. Yoshizawa, M. Chee, H. Yamashita, *Chem. Commun.* **2017**, *53*, 4677.
[24] S. P. S. Badwal, S. Giddey, A. Kulkarni, J. Goel, S. Basu, *Appl. Energy* **2015**, *145*, 80.
[25] R. Bechara, A. Gomez, V. S. Antonin, J. M. Schweitzer, F. Marechal, *Energy* **2016**, *117*, 540.
[26] Y. Li, F. Cui, M. B. Ross, D. Kim, Y. Sun, P. Yang, *Nano Lett.* **2017**, *17*, 1312.
[27] Z. L. Wang, C. Li, Y. Yamauchi, *Nano Today* **2016**, *11*, 373.
[28] C. W. Li, M. W. Kanan, *J. Am. Chem. Soc.* **2012**, *134*, 7231.
[29] M. Ma, K. Djanashvili, W. A. Smith, *Angew. Chem., Int. Ed.* **2016**, *55*, 6680.
[30] D. Raciti, K. J. Livi, C. Wang, *Nano Lett.* **2015**, *15*, 6829.
[31] F. Jia, X. Yu, L. Zhang, *J. Power Sources* **2014**, *252*, 85.
[32] K. P. Kuhl, E. R. Cave, D. N. Abramc, T. F. Jaramillo, *Energy Environ. Sci.* **2012**, *5*, 7050.
[33] S. Lee, D. Kim, J. Lee, *Angew. Chem., Int. Ed.* **2015**, *127*, 14914.
[34] H. B. Li, M. H. Yu, F. X. Wang, P. Liu, Y. Liang, J. Xiao, C. X. Wang, Y. X. Tong, G. W. Yang, *Nat. Commun.* **2013**, *4*, 1894.
[35] C. Lv, J. Sun, G. Chen, C. Yan, D. Chen, *Nano Energy* **2017**, *33*, 138.
[36] J. Nai, H. Yin, T. You, L. Zheng, J. Zhang, P. Wang, Z. Jin, Y. Tian, J. Liu, Z. Tang, L. Guo, *Adv. Energy Mater.* **2015**, *5*, 1401880.
[37] T. Yoon, K. S. Kim, *Adv. Funct. Mater.* **2016**, *26*, 7386.
[38] S. J. Li, D. Bao, M. M. Shi, B. R. Wulan, J. M. Yan, Q. Jiang, *Adv. Mater.* **2017**, *29*, 1700001.
[39] J. M. V. Nsanzimana, Y. Peng, Y. Y. Xu, L. Thia, C. Wang, B. Y. Xia, X. Wang, *Adv. Energy Mater.* **2018**, *8*, 1701475.
[40] H. J. Kim, J. K. Lee, S. Y. Shin, H. G. Jeong, D. H. Kim, J. C. Bae, *Intermetallics* **2004**, *12*, 1109.
[41] L. M. Andersen, S. Faulhaber, T. Harrington, D. C. Hofmann, H. K. Cheng, K. S. Vecchio, *J. Non-Cryst. Solids* **2017**, *469*, 70.
[42] X. Xu, A. Guo, Z. Gong, H. Du, F. Hou, J. Liu, *J. Alloys Compd.* **2017**, *701*, 645.
[43] M. C. Biesinger, L. W. M. Lau, A. R. Gerson, R. St. C. Smart, *Appl. Surf. Sci.* **2010**, *257*, 887.
[44] B. Adolphi, O. Berger, W. Fischer, *Appl. Surf. Sci.* **2001**, *179*, 102.
[45] Z. Wang, Z. Wang, W. Liu, W. Xiao, X. W. Lou, *Energy Environ. Sci.* **2013**, *6*, 87.
[46] Y. Jiang, D. Zhang, Y. Li, T. Yuan, N. Bahlawane, C. Liang, W. Sun, Y. Lu, M. Yan, *Nano Energy* **2014**, *4*, 23.
[47] S. Sun, D. Gebauer, H. Cölfen, *Chem. Sci.* **2017**, *8*, 1400.
[48] J. Wu, R. M. Yadav, M. Liu, P. P. Sharma, C. S. Tiwary, L. Ma, X. Zou, X. Zhou, B. I. Yakobson, J. Lou, P. M. Ajayan, *ACS Nano* **2015**, *9*, 5364.
[49] R. Zhang, W. Lv, L. Lei, *Appl. Surf. Sci.* **2015**, *356*, 24.
[50] S. Gao, X. Jiao, Z. Sun, W. Zhang, Y. Sun, C. Wang, Q. Hu, X. Zu, F. Yang, S. Yang, L. Liang, J. Wu, Y. Xie, *Angew. Chem., Int. Ed.* **2016**, *55*, 698.
[51] Y. Hori, H. Wakebe, T. Tsukamoyo, O. Koga, *Electrochim. Acta* **1994**, *39*, 1833.
[52] D. D. Zhu, J. L. Liu, S. Z. Qiao, *Adv. Mater.* **2016**, *28*, 3423.
[53] T. Zhang, H. Zhong, Y. Qiua, X. Lia, H. Zhang, *J. Mater. Chem. A* **2016**, *4*, 16670.
[54] Y. Chen, C. W. Li, M. W. Kanan, *J. Am. Chem. Soc.* **2012**, *134*, 19969.
[55] D. Ren, Y. Deng, A. D. Handoko, C. S. Chen, S. Malkhandi, B. S. Yeo, *ACS Catal.* **2015**, *5*, 2814.
[56] J. Rosen, G. S. Hutchings, Q. Lu, R. V. Forest, A. Moore, F. Jiao, *ACS Catal.* **2015**, *5*, 4586.
[57] Y. C. Hu, Y. Z. Wang, R. Su, C. R. Cao, F. Li, C. W. Sun, Y. Yang, P. F. Guan, D. W. Ding, Z. L. Wang, W. H. Wang, *Adv. Mater.* **2016**, *28*, 10293.
[58] D. H. Won, C. H. Choi, J. Chung, M. W. Chung, E. Kim, S. I. Woo, *ChemSusChem* **2015**, *8*, 3092.